Anisotropic continuum damage model coupled to viscoplasticity for a pressure dependent alveolar bone remodeling law

M. Mengoni, JP. Ponthot
Department of Aerospace and Mechanics, Université de Liège
Chemin des chevreuils 1, 4000 Liège - Belgium
email: mmengoni@ulg.ac.be, jp.ponthot@ulg.ac.be

Abstract— **This work proposes a phenomenological bone tissue constitutive law accounting for bone remodeling of the alveolar bone for orthodontic movements of the teeth. The proposed biomechanical constitutive law, inspired from [1], is based on a elasto-visco-plastic material coupled with Continuum anisotropic Damage Mechanics ([1] considered only the case of a linear elastic material coupled with anisotropic damage). It is here formulated as to be used explicitly for alveolar bone, whose remodeling cells, opposite to most bones, seem macroscopically to be triggered by the pressure state applied to the bone matrix. An application of the mechanical model is proposed on a 2D tooth and its surrounding parodontal tissues submitted to a tipping movement. It shows the use of a pressure dependent, anisotropic, remodeling law is necessary to obtain a global movement of the tooth if no other non linearities are considered in the problem.**

Keywords— **orthodontics, bone remodeling, biomechanics**

I. Introduction

ONE of the guiding principles in orthodontics is to gradually impose progressive and irreversible bone deformations. By optimizing load positions and intensities, orthodontic treatments can be reduced both in time and cost. This optimization requires a mechanical model of the biochemical phenomena involved and of the activated dental movement. The goal of this work is to provide a constitutive model able to simulate those coupled phenomena.

Dental movement is achieved through a biochemical process of skeletal adaptation to mechanical stimuli called bone remodeling. Therapeutic forces applied through orthodontic appliances change the physiological equilibrium. Loading of the skeletal system is thus altered and bone remodeling cells are triggered to modify the bone shape and density in order to achieve a new equilibrium and adjust the stress level. This state will be maintained until new mechanical external conditions trigger new remodeling events.

For most types of bones, remodeling processes take place in order to adjust the amount of tissue and its topology according to long term loading conditions, following what is called "Wolff's law" of bone adaptation [2], [3]. Bone resorption occurs when disuse is observed. This resorption tends to decrease the amount of bone tissue where it is of no mechanical relevance. Bone apposition occurs in overloaded conditions, in order to reinforce bone where it is necessary. Bone tissue therefore adapts its density in such a way to achieve an homeostatic state of stress. It also adapts its topology in order for the trabeculae to align along the principal stress directions. Bone remodeling therefore depends not only on the stresses intensities but also on their directions.

Contrary to the majority of bones, alveolar bone remodeling seems on a macroscopic scale to depend mainly on the pressure state [4], [5]. One can observe apposition on the tension side of a tooth when loaded with an abnormal mechanical environment, such as the one obtained with orthodontics appliances, as well as resorption on the compression side. When no non-linearities are considered in the periodontal ligament, this difference can be modeled if a pressure dependent remodeling law is used for the alveolar bone. The present work concentrates on the bone behavior during remodeling and assumes the pressure state of the bone matrix as the key stimulus to differentiate apposition and resorption in overloaded conditions.

II. Methods

On experimental basis [6], one can show that remodeling occurs to modify the density proportionately to the bone matrix density (ρ_0, density for a bone with null porosity) and as function of a remodeling rate $\dot{r}$ $[mm/s]$

$$\dot{\rho} = kS_v\rho_0\,\dot{r} \tag{1}$$

The terms kS_v accounts for the available bone specific surface area (S_v, internal surface area per unit volume, related to the density, $[mm^2/mm^3]$) as defined in [7].

This remodeling rate ($\dot{\rho}$) is shown to be a function of the deviation of a given mechanical stimulus (Ψ, function of the strain energy) from an homeostatic value ($\Psi^\star$). The remodeling process tends to reduce this deviation. In the case of alveolar bone, it is here considered as a function of the pressure.

$$\dot{r} \approx \pm c(p)(\Psi - \Psi^\star) \tag{2}$$

In order to reproduce the density change both for overload ($\Psi > \Psi^\star$) and underload ($\Psi < \Psi^\star$) of the alveolar bone, the

parameter c has to be positive in underuse and a function of the pressure state in overuse (positive in compression and negative in traction).

The change in density can be translated into a change in mechanical properties (Young's modulus E and Poisson's ratio ν) through a commonly accepted law :

$$\begin{aligned} E &= B(\rho)\rho^{\beta(\rho)} \\ \nu &= \nu(\rho) \end{aligned} \tag{3}$$

A. Model

As proposed in [8], the change in elastic properties due to remodeling can be integrated in an adaptative elasticity framework. However, this supposes the bone matrix as an elastic solid and is therefore limited to low strain levels. Doblaré and co-workers [1] proposed to formulate the previous set of equations within the Continuum Damage Mechanics framework, using an energy equivalence approach of damage. In the case of bone remodeling, damage can be understood as a measure of the void volume fraction inside the bone tissue. The measure of damage used is therefore virtual and actually reflects the bone density that can evolve (Equ.1). There is no actual damage in the tissue. The undamaged material is the ideal situation of bone with null porosity and perfect isotropy. The process of bone resorption corresponds to the classical damage evolution concept, since it increases the void fraction (porosity) and therefore damage (decreases the density). However, bone apposition can reduce damage and lead to bone repair, which has to be adequately considered in this extended damage theory. Damage repair can be considered here because the total energy dissipation includes biological dissipation due to metabolism on top of the mechanical dissipation which is negative for damage repair.

Equ.(1) can therefore be formulated as a damage variation function. This formulation allows Doblaré and co-workers in [1] to extend the density variation to an anisotropic formulation, using an anisotropic damage variable. Directionality therefore follows the idea suggested by Cowin [9] and links the anisotropic damage tensor to the fabric tensor. The use of the continuum damage theory allows to define independently the internal variables such as density and mechanical properties. It therefore is an improvement of the anisotropic extension of [6] which was proposed in [10]. Indeed, in [10], Jacobs and co-workers used a global optimization function to define the remodeling stimulus and therefore the internal variables were not independent. Even though the continuum damage formulation solves this difficulty, Doblaré and co-workers limited their approach in [1] to an elastic bone matrix as was done in [8]. In its isotropic formulation Doblaré's model therefore uses the following set of equations :

$$\text{effective strain} : \tilde{\varepsilon} = (1-d)\varepsilon \tag{4}$$

$$\text{effective stress} : \tilde{\sigma} = \frac{\sigma}{(1-d)} \tag{5}$$

$$\text{constitutive law} : \tilde{\sigma} = \mathbb{C}_0 : \tilde{\varepsilon} \tag{6}$$

$$\text{damage variation} : \dot{d} = f(d, \sigma, \dot{r}, \rho_0) \tag{7}$$

with d an isotropic damage variable, $\mathbb{C}_0$ Hooke's tensor for the undamaged material.

We propose to extend the model stated in [1] to a more generalized mechanical behavior of the bone matrix, considering it as an elasto-visco-plastic material. This model is also adapted to account for an explicit pressure dependence of the remodeling rate in the alveolar bone.

In order to couple continuum damage and plasticity, the use of a strain equivalence approach, relating the stress level in the damaged material with the stress in the undamaged material that leads to the same strain, is chosen. This approach keeps the physical definition of damage as related to the surface density of defects, opposite to the energy equivalence approachused in [1] because of its difference between strain and effective strain. The plasticity is therefore simply coupled to damage by expressing the plastic criterion in term of effective stresses instead of stresses. In its isotropic formulation the proposed model therefore uses the following set of equations :

$$\text{effective stress} : \tilde{\sigma} = \frac{\sigma}{(1-d)} \tag{8}$$

$$\text{constitutive law} : \overset{\triangledown}{\tilde{\sigma}} = \mathbb{M}_0 : E \tag{9}$$

$$\text{damage variation} : \dot{d} = f(d, \sigma, \dot{r}, \rho_0) \tag{10}$$

with d an isotropic damage variable, $\mathbb{M}_0$ an elasto-plastic material tensor for the undamaged material, E the strain rate (energy conjugated to the stress tensor, in a large deformation framework) and where the $\triangledown$ sign accounts for an objective time derivative.

When extending the strain equivalence approach (Equ.8-10) to anisotropic damage, according to Lemaitre and Desmorat [11], [12], one of the only effective stress ($\tilde{\sigma}$) definition that fulfills the conditions of being symmetric, compatible with the thermodynamics (existence of a stress potential) and that can express different effects on the hydrostatic and deviatoric behavior (by means of an hydrostatic sensitivity parameter, η) is represented by

$$\tilde{\sigma} = \mathtt{dev}(HsH) + \frac{p}{1-\frac{\eta}{3}D_{kk}}I = \tilde{s} + \tilde{p}I \tag{11}$$

where s and p are respectively the stress deviator and the pressure and where $H = (I-D)^{-1/2}$ is a second order

symmetric tensor (called in this work the remodeling tensor), D being symmetric (as an extension of the isotropic damage variable, d).

The damage evolution is thermodynamically associated to the elastic strain energy Φ^{el} which can be written, considering an isotropic matrix (the elasticity parameters are of the number of two, the bulk modulus, K, and the shear modulus, G) as :

$$2\Phi^{el} = \frac{1}{2G}\mathtt{tr}(Hs^{el}Hs^{el}) + \frac{p^{el\ 2}}{K(1-\frac{\eta}{3}D_{kk})} \tag{12}$$

An external mechanical stimulus, Y, is identified with the variable thermodynamically associated with the remodeling tensor H, choosing to use the stress as the external driving force, giving :

$$Y = \frac{\partial \Phi^{el}(\sigma, H)}{\partial H} \tag{13}$$

It is obtained in terms of the external independent variable (stress) and the internal variable (remodeling tensor or damage tensor) as

$$Y = -2\left[\frac{1}{K}\frac{\eta p^2}{3-\eta\mathtt{tr}(D)}H^{-3} + \frac{1}{2G}sHs\right] \tag{14}$$

If the remodeling criteria are chosen as in [1], one can show after a few calculation that

-for bone formation :

$$\overset{\triangledown}{H} = -\frac{3\beta k S_v \dot{r}}{2\mathtt{tr}(H^{-2}(J\mathbb{W})H)}\frac{\rho_0}{\rho}J\mathbb{W} \tag{15}$$

-for bone resorption :

$$\overset{\triangledown}{H} = -\frac{3\beta k S_v \dot{r}}{2\mathtt{tr}(H^{-2}(J^{-3}\mathbb{W})H)}\frac{\rho_0}{\rho}J^{-3}\mathbb{W} \tag{16}$$

with $\mathbb{W}$ a fourth order unit anisotropic tensor,
$J = \frac{1}{3}(1-2w)\mathtt{tr}(Y)I + wY$ and $w \in [0,3]$ can be related to $\eta \in [1,\infty[$ as a measure of the hydrostatic sensitivity.

The remodeling rate $\dot{r}$ is expressed, in its pressure dependent formulation, as :

$$\dot{r} = \begin{cases} c_f g_o & \text{if } g_o \geq 0,\ g_u < 0 \quad \text{and} \quad p > 0 \\ -c_r g_o & \text{if } g_o \geq 0,\ g_u < 0 \quad \text{and} \quad p < 0 \\ 0 & \text{if } g_o < 0,\ g_u < 0 \\ -c_r g_u & \text{if } g_u \geq 0,\ g_o < 0 \end{cases}$$

where c_r and c_f are two remodeling constants respectively for bone formation and bone resorption, p is the pressure (positive in tension) and g_o and g_u are the remodeling criteria (same units as the one of stresses) respectively for bone overload and bone underload used in [1] and expressed for a strain equivalence approach in continuum damage mechanics. These criteria express the deviation of the mechanical stimulus Ψ from its homeostatic value.

- overload criterion : $g_o \propto \Psi - (1+\Omega)\Psi^\star < 0$
- underload criterion : $g_u \propto 1/\Psi - 1/((1-\Omega)\Psi^\star) < 0$

The parameter Ω introduced in these definition accounts for a lazy zone. This is an interval around the homeostatic level for which no remodeling process takes place. The mechanical stimulus used is a function of the strain energy (through the external mechanical stimulus Y) at tissue level and the number of loading cycles considered in the time integration. It is expressed at the tissue level supposing stress in the tissue can be related to continuum stress through a proportionality coefficient experimentally shown to be the square of the reduced density [10] : continuum stress = $(\rho/\rho_0)^2 \times$tissue level stress.

Coupling with plasticity can be done assuming an additive decomposition of the strain rate :

$$E = E^{el} + E^{pl} \tag{17}$$

where E^{el} follows Hooke's law :

$$\overset{\triangledown}{\tilde{\sigma}} = \mathbb{C}_0 E^{el} \tag{18}$$

and E^{pl} can be calculated through the normality rule on the plastic criterion (associated plasticity) expressed in term of effective stresses.

When Von-Mises criterion is chosen (although it is clear that the relevant inelastic processes are different from that of classical plasticity), it results for isotropic hardening in :

$$E^{pl} = \frac{3}{2}\frac{\dot{\lambda}}{\tilde{\sigma}_{eq}}\mathtt{dev}(H\tilde{s}H) \tag{19}$$

where $\tilde{\sigma}_{eq}$ is the equivalent stress used for the Von-Mises criterion

$$\tilde{\sigma}_{eq} = \sqrt{\frac{3}{2}\tilde{s} : \tilde{s}} \tag{20}$$

and λ a flow parameter. This choice of criterion assumes that only shear stresses are responsible for plastic strains. As both remodeling triggering and damage variation are function of the pressure value, this assumption may be too restrictive.

This formulation is integrated in a finite element code (home made code Metafor [13]) using the following time-step integration : starting from a known stress state (s, p) and remodeling tensor (H), plasticity is computed using effective stresses ($\tilde{s}$, $\tilde{p}$) with a constant remodeling tensor, giving plastic deformations and final stresses. Damage evolution is then computed and a new remodeling tensor is determined. Stresses and plastic deformations are then re-evaluated, up to convergence of the updated remodeling

tensor (see [14] for details on the method). A consistent tangent operator has also been developed for this theory when integrated in an iterative process as the one exposed.

B. Application

We consider the potential of the pressure dependent model to predict the density evolution of alveolar bone tissue. As an example, we present a 2D model (plane strain state) of the parodontal tissue of a rigid tooth. The aim is to predict the bone density and its evolution from initial ideal situations (for both the geometry and the mechanical behavior) with given displacements that characterize the orthodontic appliances.

The root is parabolic and surrounded by a constant thickness ($0.2mm$) periodontal ligament (PdL) as well as trabecular and cortical bone [15]-[18]. It is of $12.6mm$ in height and $6mm$ in width at the collar. The ligament is surrounded by a trabecular bone of arbitrary variable thickness and a cortical layer of around $0.5mm$ in width (see Fig. 1).

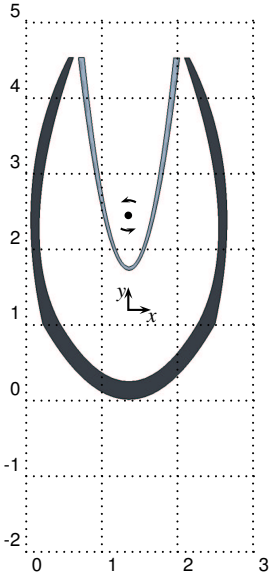

Fig. 1. Geometry - light gray : periodontal ligament, dark-gray : cortical layer, in between : alveolar bone. The dot represents the center of rotation

The PdL and cortical layer mechanical behaviors [15]-[18] are chosen elastic ($E_{\text{pdl}} = 0.6MPa$, $\nu_{\text{pdl}} = 0.45$, $E_{\text{cor}} = 16GPa$, $\nu_{\text{cor}} = 0.3$). The trabecular bone mechanical behavior is elasto-plastic with the proposed continuum damage model. The damage evolution follows the remodeling law proposed in this work.

Neither this problem nor the starting situations are "real" problems, therefore, the homeostatic values are not relevant (as well as the other parameters of the model, especially for a qualitative evaluation). A quasi-static loading is performed, the time-unit of the simulation is therefore also of no relevance.

In order to test the anisotropic behavior, we present four simulations.

The first two tests consider initial damage in only one direction (either along the vestibulo-lingual direction, x or along the root axis, y), both other initial damage values being set to zero. The non null initial damage is set to .9. It therefore corresponds to a mean initial damage of .3, getting a density of $1.9g/cc$, a porosity of 10% and a stiffness of $13GPa$ (calculated from the strain equivalence damage definition in case of isotropy : $d = 1 - \frac{E}{E_0}$ with E_0 the stiffness obtained for a bone of null porosity, $E_0 = 18.5GPa$). These values for density and stiffness are much higher than what they should be in a realistic test, for which the mean damage value would be around .8. However, this set of tests is proposed for the sake of comparison to analyze the anisotropic behavior of the model. The two other tests present the same initial mean damage chosen to be .3 : the third one considers an initial bone as isotropic with a uniform density distribution ; the last test considers initial damage in the geometry plane (x,y). We therefore get an initial damage in the two plane directions of .45 while it is zero on the third direction.

Remark 1 An initial damage considered only along the y axis corresponds to trabeculae of the alveolar bone aligned along the the tooth main axis and perpendicular to the main direction of movement. However initial damage only along the x axis corresponds to a bone whose trabeculae are aligned perpendicularly to the root axis along the direction of movement. Damage evolution for both these cases would therefore be dissimilar, allowing a greater damage variation for damage along the y axis than along the x axis as the trabeculae because the movement is perpendicular to the fibers main direction. **[end of remark]**

A tipping movement is applied to the tooth root with a center of rotation situated at $3mm$ from the root apex, i.e. below one third of the root length (see Fig. 1) as proposed in [19] among others. Tipping is kept to obtain an angle of two degrees with the vertical axis, the basal bone being fixed. As the root and surrounding tissues are symmetric, the rotation direction is of no relevance. Getting from an angle of zero to the final angle is done is 10 time units and this angle is kept for a remaining 90 time units. Damage variation is observed during this constant displacement period.

III. Results

A. Model

The discussion on the model characteristics that follows is done on the isotropic formulation of the model in order to decouple the effects due to the remodeling rate function and to the orientation of the structure.

As no more dependence on the orientation has to be represented, one can write $H = hI$, $w = 0$ and $\eta = 1$, both criteria g_o and g_u take a simple formulation given by :

$$g_o = U - (1+\Omega)U^\star < 0 \quad (21)$$

$$g_u = 1/U - 1/((1-\Omega)U^\star) < 0 \quad (22)$$

where U is expressed in Equ.(23) and $U^\star$ is a reference homeostatic value of U.

$$U(d,\tilde{\sigma}) \propto (1-d)^{3/4}\sqrt{2\bar{u}(\tilde{\sigma})} \quad (23)$$

where $d = 1 - h^{-2}$ as in the strain equivalence approach and $\bar{u}$ is the effective elastic energy density (as also defined in [11], establishing the basis of the CDM theory, and accounting for the stress triaxiality) :

$$\bar{u}(\tilde{\sigma}) = \int \tilde{\sigma} : d\tilde{\varepsilon}^{el} = \frac{\tilde{J}_2^2}{2E}\left[\frac{2}{3}(1+\nu) + 3(1-2\nu)\frac{\tilde{p}^2}{\tilde{J}_2^2}\right] \quad (24)$$

with $\tilde{J}_2 = \sqrt{\frac{3}{2}\tilde{s}_{ij}\tilde{s}_{ij}} = \frac{1}{1-d}\sqrt{\frac{3}{2}s_{ij}s_{ij}}$, s being the deviatoric stress tensor.

Finally, Equ.(15) and (16) both lead to the same damage variation (see Fig. 2), with $\dot{r}$ as defined by Equ.(17):

$$\dot{d} = -\beta k S_v \dot{r}\frac{\rho_0}{\rho}(1-d) \quad (25)$$

This damage variation is nothing but the expression of Equ (1) in term of the damage variable. As damage variation is positive for resorption and negative for formation, we can detect on Fig 2 different remodeling zones as well as the lazy zone as a function of damage. As expected through the introduction of the specific surface S_v, damage variation for values of damage close to 1.0 tend to high (negative) values but is reduced to zero for full damage (not on the figure). In resorption, although the remodeling rate increases (in absolute value) for a damage decay, damage variation does not reach high values due to the tendency of the specific surface to decrease faster than the remodeling rate increases. The discontinuity of damage variation for a damage value of about 0.83 is due to the slight slope discontinuity introduced by the particularization of Equ.(3) in the definition of bone Young's modulus (as in [20]).

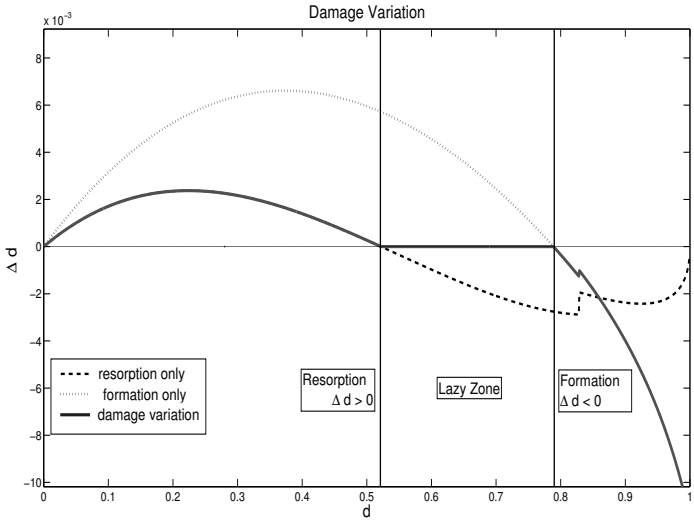

Fig. 2. Damage variation as a function of damage for a positive pressure

Once the remodeling model has been formulated, we need to check its ability to achieve qualitative results close to the ones obtained in experimental tests of actual alveolar bone. This is accomplished in the next section in which the model is applied to the study of the remodeling behavior in the alveolar bone submitted to orthodontic treatments with the four simulations presented earlier.

B. Application

Tipping movement of a tooth is obtained with displacement controlled simulations, the angle of rotation being increased from zero to two degrees in ten time-steps.

If the whole movement was rigid around the center of rotation, one would expect a displacement, due to the rigid rotation, at the collar of $-.33mm$ horizontally and $\pm.11mm$ vertically. However, as the bone is fixed at its base and as the rotation leads to deformation of the periodontal ligament as well as the bone, the movement actually observed leads to smaller displacements at the collar (see 4).

The mean damage evolution is shown in Fig.3 for each simulation on three sets of points (two at the apex, two at the collar and two at mid-height of the root - above the center of rotation) situated symmetrically around the root axis and adjacent to the periodontal ligament.

Observation 1 The mean damage variation observed is abrupt during loading of the tooth and tends to stabilize towards an equilibrium mean damage value when the angle of rotation is kept constant. For most cases, the variation during the constant displacement is in the same direction as the initial variation as the pressure state stays the same during the whole simulation. However, for the root mid-height this changes when damage is initially on the x direction only (see **observation 3** for explanation). **[end of observation]**

Observation 2 Damage variation at the collar is much less than at the apex or along the root for all four simulations and on both sides of the root main axis. Indeed the tipping movement leads to smaller shear and hydrostatic stresses at the collar than along the root ($J_2^{\text{collar}} \approx 1MPa$, $J_2^{\text{root}} \approx 3MPa$, $p^{\text{collar}} \approx .2MPa$, $p^{\text{root}} \approx 1-3MPa$). It also

gives a ratio hydrostatic stress to shear stress (used in the definition of $\bar{u}$, Equ.24) of .2 at the collar while it is of around 1 to 3 along the root. Therefore, the value of the external mechanical stimulus Y is smaller at the collar than along the root. The remodeling rate is also smaller because even tough reducing Y reduces Ψ, its value stays above its homeostatic value $\Psi^\star$ and overloaded conditions are still observed at the collar, $\dot{r}$ is therefore reduced and so is damage variation. **[end of observation]**

Observation 3 For each set of points, while overloaded conditions are kept for all simulations, one can see apposition on one side (reduction of mean damage) and resorption on the other (increase of mean damage). All points are therefore subjected, for the same vertical location, to traction on one side of the tooth and compression on the other. Nevertheless, one point can be submitted either to traction or to compression according to the initial anisotropy of damage.

For the root mid-height, the labial side is in compression (increase of damage) except for the simulation with initial damage on the x direction only for which the labial side is in traction. This can be explained as follows. As the tipping movement is a rotation along a center of rotation situated at one third of the root length (starting from the apex), there is a pressure gradient on each side of the root axis. On the labial side, the bone is in compression at the apex and in traction at the collar. On the lingual side, it is in traction at the apex and in compression at the collar. However, the change of pressure sign is not observed at the same vertical location for all four simulations. One will get most of the bone surrounding the root in traction on the lingual side when the initial damage is considered as fully isotropic or as non-zero on both plane directions while around two thirds are in traction for initial damage on the y direction and only one half is in traction for initial damage on the x direction. Therefore the pressure state at mid-height is in traction on the lingual side for the first three simulations while it is in compression for the last one.

The collar shows almost no damage variation for initial damage considered isotropic or on the two plane directions. Even tough mean initial damage is equal for all simulations, local values of damage are smaller for these two simulations than for the others and, as exposed earlier, stress intensities are smaller as well. Therefore, the remodeling rate is quite small and so is the mean damage variation.

The change in damage variation behavior at the collar between the two mono-directional damage simulations is explained in the same way as the change of behavior at the root mid-height.

However, at the apex, for all simulations, the points are either in traction or in compression on each side of the

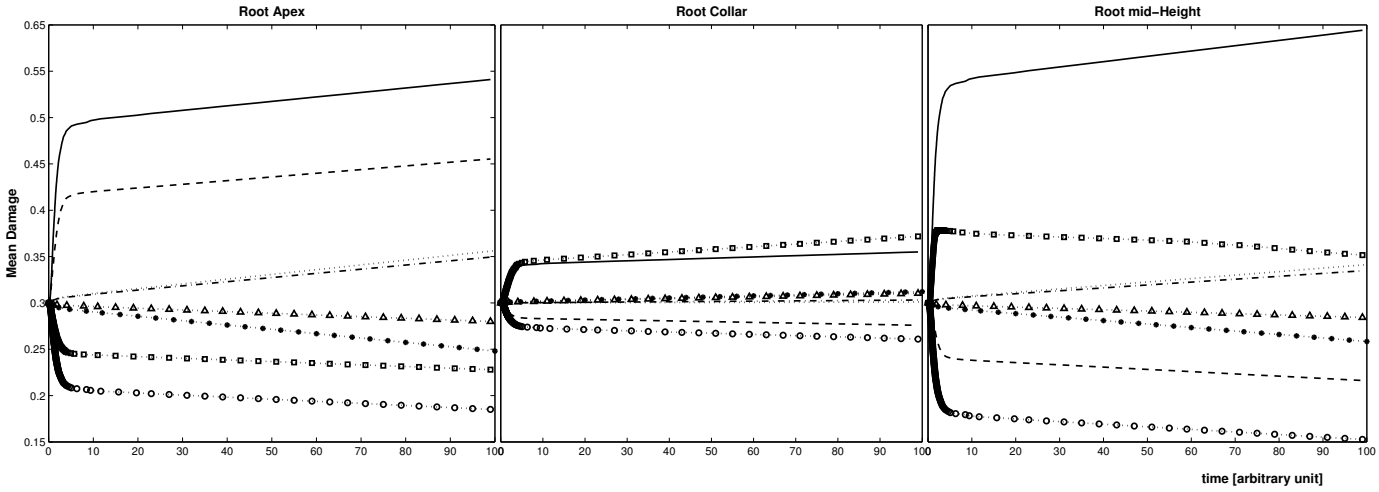

Fig. 3. MEAN DAMAGE COMPARISON ON THREE SETS OF POINTS : On all graphs, test with initial damage on x is in dashed line (labial side) and squares (lingual side), test with initial damage on y in plain line (labial side) and circles (lingual side), test with initial damage on the x,y plane is in dashed-dotted line (labial side) and triangle (lingual side) and test with initial isotropic damage is in dotted line (labial side) and plain circles (lingual side). The left graph is for two points situated at the apex, the labial side in compression and lingual side in traction, the middle graph for points at the collar, the labial side in traction and lingual side in compression, and the right graph at the root mid-height, the labial side in compression and lingual side in traction. On three cases, the points are situated symmetrically around the root axis, adjacent to the periodontal ligament. An angle of 2 degrees is obtained within the first ten time-steps and kept up to a hundred time-steps.

tooth. Damage variation is therefore qualitatively the same for all simulations. **[end of observation]**

Observation 4 As expected in Remark 1, both for the root mi-height and the root apex, mean damage variation for simulation with damage only on the x direction or only on the y direction, do not present the same order of values. Ratio between mean damage variation for the x initial damage simulation and the y one is about 1.5 at the root apex while it is about 5 at the mid-height. This is due to the alignment of the tissue fibers with the loading for the x initial damage simulation while fibers are perpendicular to loading on the other case. This difference in damage variation is not present at the collar because the bone width at that location is much smaller and loading lines more oblique to the fibers than lower on the root. **[end of observation]**

This set of observations shows that using an anisotropic model is quite necessary to describe bone remodeling as it allows, for a given mean damage value, to obtain different damage variation, both in intensity and repair/damaging behavior.

If a non pressure dependency was used for the remodeling rate coefficient in overload conditions, there would be no difference observed between the labial and lingual side of the tooth for each set of points. Therefore, each location would undergo apposition on both sides of the tooth (damage repair) and only bone growth would be observed. This would lead without any doubt to jaw problems maybe up to extrusion of a tooth. Therefore, a model not accounting for a non linear periodontal ligament mechanical law has to include a pressure dependency for the remodeling coefficient such as the one proposed. This pressure dependency could be avoided if the periodontal ligament mechanical law would lead to mechanical stimuli (proportional to the strain energy density) of the bone that would be smaller or larger than its homeostatic value according to pressure sign. The pressure dependency of the model would therefore be at the ligament level and not at the bone remodeling one.

IV. Conclusions

The present study introduces a numerical model for the simulation of orthodontic tooth movement based on the assumption that bone remodeling processes during tooth movement are controlled by elastic energy density as well as pressure state of the alveolar bone. In spite of the necessary idealizations, the proposed phenomenological description of bone remodeling specified for alveolar bone allows to qualitatively represent density variation of the bone surrounding a tooth when submitted to loading representing orthodontic appliances. The need to use a pressure dependent remodeling rate is shown to be useful to represent tooth movement as long as the periodontal ligament is supposed not to be dependent on the pressure state. This hypotheses may be too restrictive but has yet to be shown not valid as the use of an appliance would most of the time increase the strain energy on all sides of the tooth root.

We present in details an analysis of the importance to use an anisotropic damage as well as on the importance of the initial anisotropy considered. As damage represent density of the bone, anisotropy of damage represent trabeculae orientation. The initial anisotropy of damage depends on the trabeculae organization of the alveolar bone due to physiological equilibrium. It therefore is patient dependent and the need of an evaluation of the bone state previous to treatment is necessary if any optimization of treatment was to be considered. This evaluation should give the possibility to assess the fabric tensor of the bone tissue of the jaw. This fabric tensor is directly linked to the anisotropy and as proposed in [1] can be linked to the remodeling tensor.

Further work should consider an application of this remodeling law to a patient specific model, not only for the initial damage considered but mainly for the geometry of the problem as well as for various types of appliances and loading.

Acknowledgments

The authors would like to acknowledge Dr. PP Jeunechamps for his enlightenment on damage mechanics and the formulation of its coupling to plasticity Prof. M. Limme of the Orthodontics Department, for his suggestions as well as Prof. R. Charlier.

References

[1] M. Doblaré and J. M. García, "Anisotropic bone remodelling model based on a continuum damage-repair theory," *J. Biomech.*, vol. 35, no. 1, pp. 1–17, Jan 2002.

[2] S. C. Cowin, "Tissue growth and remodeling," *Annu Rev Biomed Eng*, vol. 6, pp. 77–107, 2004.

[3] W. E. Roberts, "Bone physiology of tooth movement, ankylosis, and osseointegration," Seminars in Orthodontics, 2000, Volume 6, Issue 3, September 2000, Pages 173-182.

[4] C. Bourauel, D. Freudenreich, D. Vollmer, D. Kobe, D. Drescher, and A. Jäger, "Simulation of orthodontic tooth movements. a comparison of numerical models," *J. Orofac. Orthop.*, vol. 60, no. 2, pp. 136–151, 1999.

[5] B. Melsen, "Tissue reaction to orthodontic tooth movement–a new paradigm," *Eur. J. Orthod.*, vol. 23, no. 6, pp. 671–681, Dec 2001.

[6] G. S. Beaupré, T. E. Orr, and D. R. Carter, "An approach for time-dependent bone modeling and remodeling–theoretical development," *J. Orthop. Res.*, vol. 8, no. 5, pp. 651–661, Sep 1990.

[7] R.B. Martin, "Porosity and specific surface of bone," *Crit. Rev. Biomed. Eng.*, vol. 10, no. 3, pp. 179–222, 1984.

[8] S. C. Cowin and D. H. Hegedus, "Bone remodeling i: theory

of adaptive elasticity," *Journal of Elasticity*, vol. V6, no. 3, pp. 313–326, July 1976.

[9] S. C. Cowin, R. T. Hart, J. R. Balser, and D. H. Kohn, "Functional adaptation in long bones: establishing in vivo values for surface remodeling rate coefficients," *J. Biomech.*, vol. 18, no. 9, pp. 665–684, 1985.

[10] C. R. Jacobs, J. C. Simo, G. S. Beaupre, and D. R. Carter, "Adaptive bone remodeling incorporating simultaneous density and anisotropy considerations," *J. Biomech.*, vol. 30, no. 6, pp. 603–613, June 1997.

[11] J. Lemaitre and R. Desmorat, *Engineering Damage Mechanics: Ductile, Creep, Fatigue and Brittle Failures*, Springer, 2005.

[12] R. Desmorat and S. Otin, "Cross-identification isotropic/anisotropic damage and application to anisothermal structural failure," *Engineering Fracture Mechanics*, vol. 75, pp. 3446–3463, 2008.

[13] Metafor, *A large strain finite element code*, LTAS - MN2L / University of Liège, http://metafor.ltas.ulg.ac.be/ , 2009.

[14] P.P. Jeunechamps, *Simulation numérique, à l'aide d'algorithmes thermomécaniques implicites, de matériaux endommageables pouvant subir de grandes vitesses de déformation. Application aux structures aéronautiques soumises à impact*, Phd thesis, University of Liège (Belgium), School of Engineering, Aerospace and Mechanics Department, 2008.

[15] C. Bourauel, D. Vollmer, and A. Jäger, "Application of bone remodeling theories in the simulation of orthodontic tooth movements," *J. Orofac. Orthop.*, vol. 61, no. 4, pp. 266–279, 2000.

[16] P. D. Jeon, P. K. Turley, and K. Ting, "Three-dimensional finite element analysis of stress in the periodontal ligament of the maxillary first molar with simulated bone loss," *Am. J. Orthod. Dentofacial Orthop.*, vol. 119, no. 5, pp. 498–504, May 2001.

[17] H. Qian, J. Chen, and T. R. Katona, "The influence of pdl principal fibers in a 3-dimensional analysis of orthodontic tooth movement," *Am. J. Orthod. Dentofacial Orthop.*, vol. 120, no. 3, pp. 272–279, Sep 2001.

[18] J. Schneider, M. Geiger, and F.-G. Sander, "Numerical experiments on long-time orthodontic tooth movement," *Am. J. Orthod. Dentofacial Orthop.*, vol. 121, no. 3, pp. 257–265, Mar 2002.

[19] D. Vollmer, C. Bourauel, K. Maier, and A. Jäger, "Determination of the centre of resistance in an upper human canine and idealized tooth model," *Eur. J. Orthod.*, vol. 21, no. 6, pp. 633–648, Dec 1999.

[20] C. R. Jacobs, *Numerical simulation of bone adaptation to mechanical loading*, Ph.D. thesis, Department of Mechanical Engineering.Stanford University, 1994.